

NASA Technical Memorandum

NASA TM-86541

A COMPUTATIONAL STUDY OF MULTIPLE JET
AND WALL INTERACTION

By Warren Campbell

Systems Dynamics Laboratory

February 1986

(NASA-TM-86541) A COMPUTATIONAL STUDY OF
MULTIPLE JET AND WALL INTERACTION (NASA)
13 p HC A02/MF A01

CSCL 20D

N86-24937

Unclas

G3/34 43348

NASA

National Aeronautics and
Space Administration

George C. Marshall Space Flight Center

TABLE OF CONTENTS

	Page
INTRODUCTION	1
PREBURNER MODEL	3
EFFECT OF UPSTREAM BOUNDARY CONDITIONS	4
MESH DEPENDENCY	7
SUMMARY	7
REFERENCES	8

LIST OF ILLUSTRATIONS

Figure	Title	Page
1.	Baffle and injector configuration for the fuel preburner.....	1
2.	Erosion patterns in the fuel preburner suggestive of the Coanda effect.....	2
3.	Model preburner showing boundary conditions and sample uniform recirculation zone calculation	3
4.	Preburner flow for $turb = 0.01$	5
5.	Preburner flow for $turb = 0.001$	6
6.	Recirculation zone length as a function of the upstream boundary condition on turbulent kinetic energy	6

TECHNICAL MEMORANDUM

A COMPUTATIONAL STUDY OF MULTIPLE JET AND WALL INTERACTION

INTRODUCTION

Combustion of hydrogen and oxygen in the preburner of the High Pressure Fuel Turbopump of the Space Shuttle Main Engine drives the turbine and energizes the pump which circulates hydrogen fuel through the engine. The fuel preburner has 264 coaxial injector elements and three baffles (Fig. 1).

Erosion patterns on the preburner faceplate and baffles suggest that the injector jets have attached to the walls. Examples of this type of erosion are given in Figure 2. The preburner operates in a very fuel rich condition and efforts are made to keep combustible oxygen away from walls by using sheets of hydrogen.

The fluid in the outer concentric jet of each injector element is hydrogen. In most instances, baffle or wall discoloration or erosion have been attributed to this outer hydrogen sheet being disrupted by contamination lodged in the narrow clearance between the inner and outer annuli of the injector. In some cases, the obstructing contamination was located during visual inspection. In other instances, no contamination was apparent.

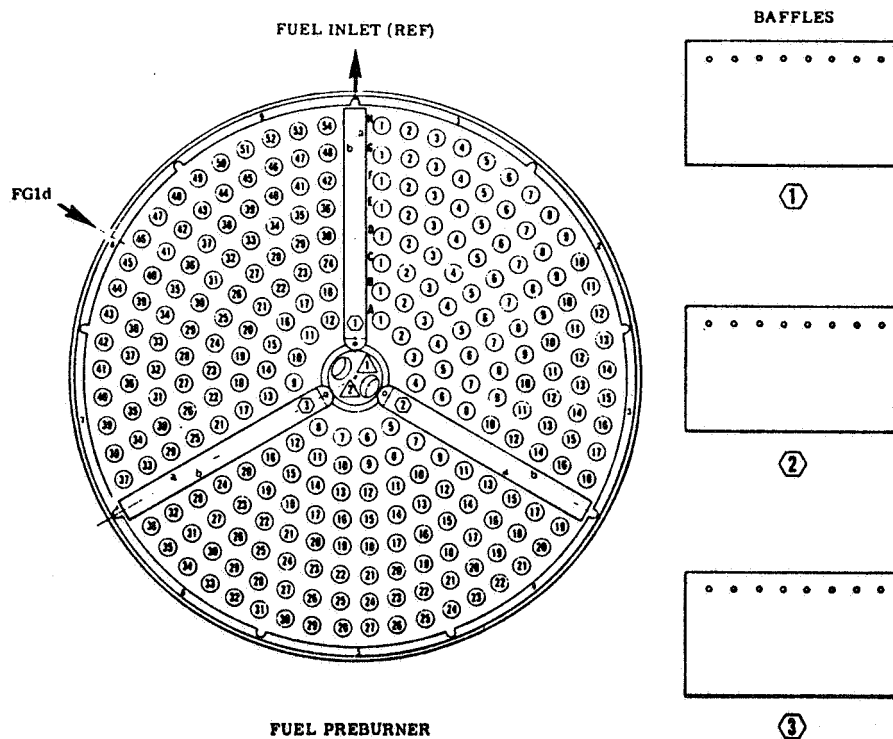
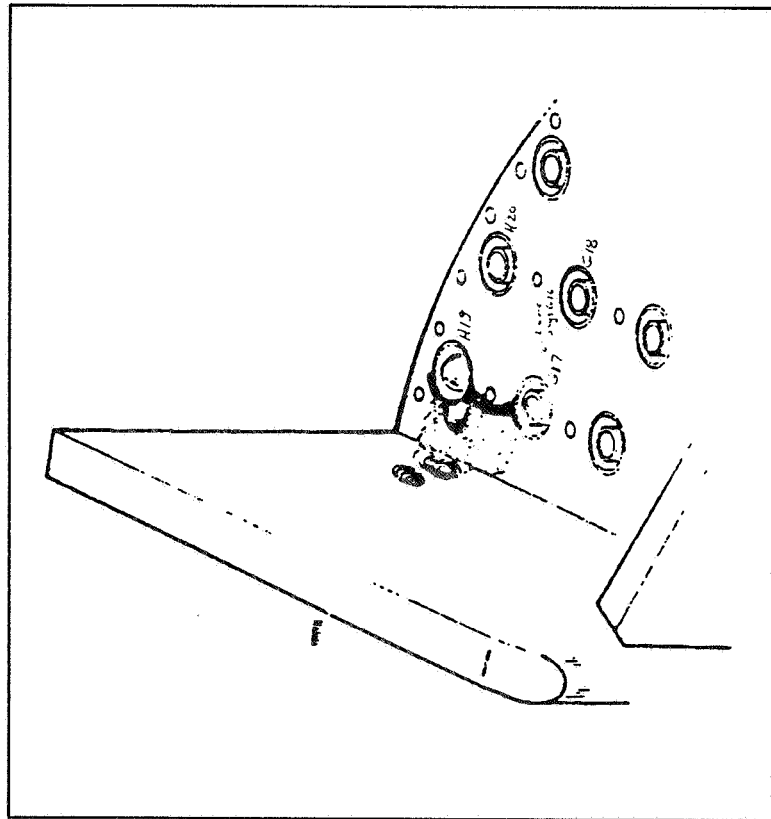


Figure 1. Baffle and injector configuration for the fuel preburner.

STS-3



ENGINE 2014

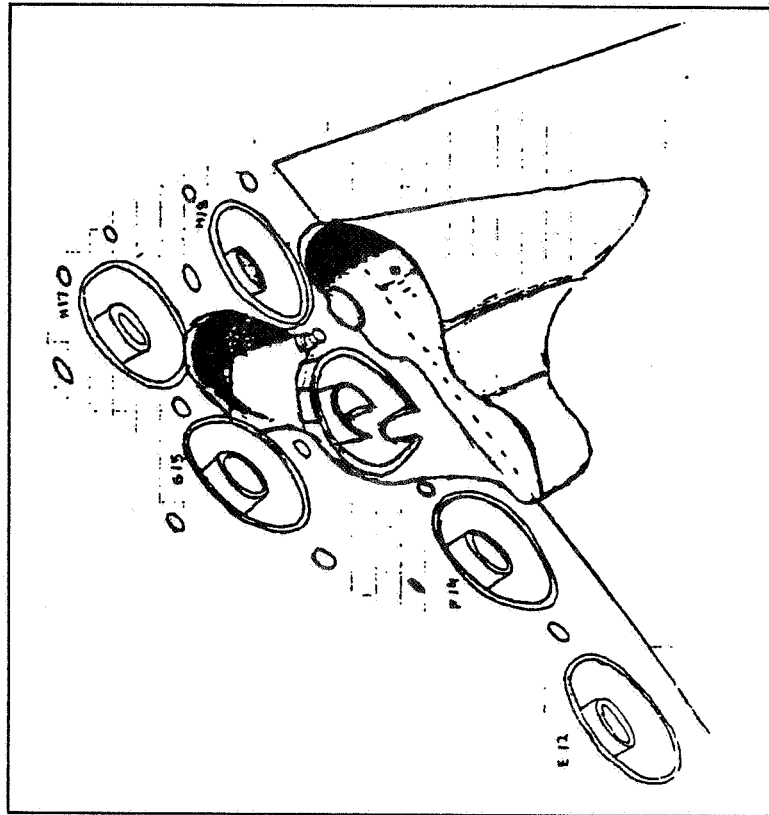


Figure 2. Erosion patterns in the fuel preburner suggestive of the Coanda effect.

When significant erosion occurs, repairs are made on faceplate and baffles and the central, oxygen-injector region is plugged permanently. In the course of testing the development engines, a number of the injector elements may be pinned shut. At present, all six of the outer wall-baffle corner-injector elements (H1, H18, H19, H36, H37, and H54) are pinned before testing. In the course of testing, wear and erosion make the pinning of additional injector elements necessary. As more and more are pinned, erosion becomes more likely. Because each central injector element is fed upstream by a common oxygen supply manifold, the normal flow through pinned elements is rerouted through the other unpinned elements. This causes the injector elements to operate in a more oxygen rich mode making the remaining unplugged injectors burn hotter and erosion more likely.

This study was initiated to investigate the possibility that contamination might not always be required to cause wall and baffle erosion. Jet attachment to adjacent walls, i.e., the Coanda effect, is studied as an alternative mechanism.

PREBURNER MODEL

A two-dimensional "preburner" consisting of three jets, a baffle, and symmetry boundaries are investigated. Figure 3 depicts the boundary conditions and a sample calculation. Computational modeling was done with a version (PHOENICS) of the Patankar Spalding algorithm [1] with upwind differencing. Reynolds number of the incoming jets, based on jet diameter, was 6,000,000. Turbulent closure was accomplished using the $k-\epsilon$ model with wall functions [2].

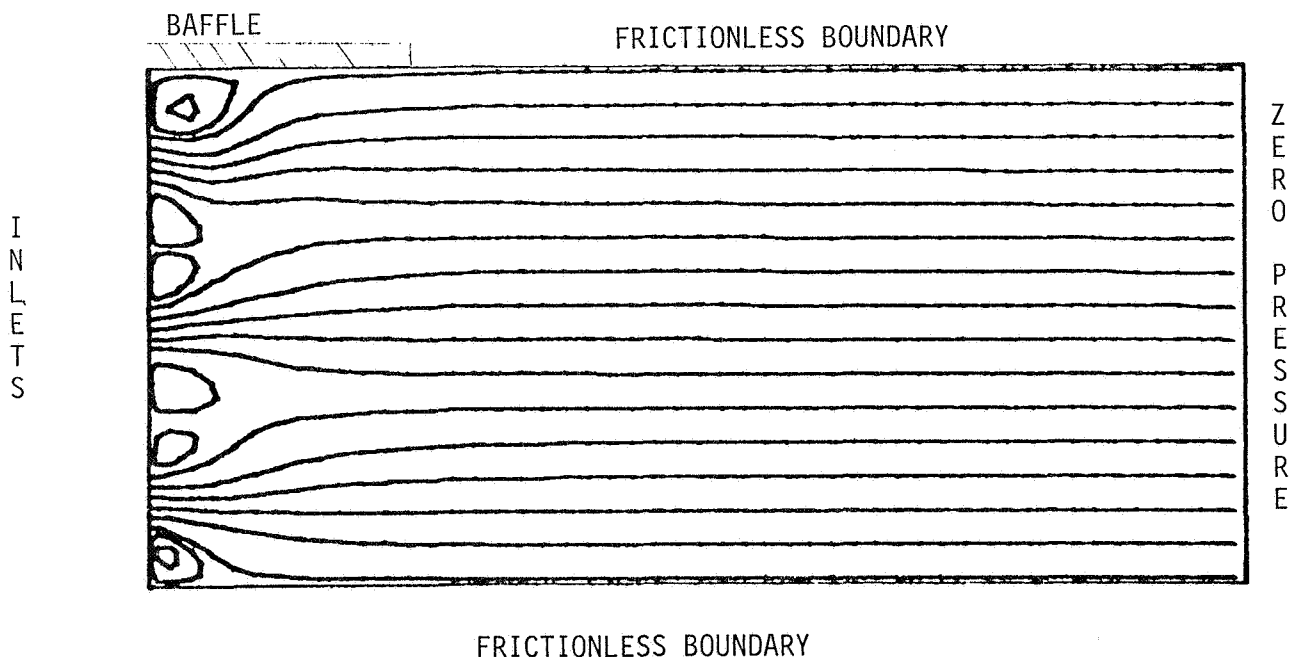


Figure 3. Model preburner showing boundary conditions and sample uniform recirculation zone calculation.

Referring to Figure 3, the dimensions of the flow field were 3.95 cm by 25 cm. The baffle was 5 cm long. The incoming jet diameters were 0.4 cm. In all of the streamline depictions in this paper, the cross-stream dimension is expanded by a factor of three to enhance clarity. Downstream of the baffle and on the upper boundary, the wall is frictionless. The lower wall is a frictionless, symmetry boundary. Downstream, a zero pressure boundary condition was imposed. In a companion study by Don Bai and S. T. Wu still in progress, the inlet jet velocity was varied, but for this study was fixed at 30 m/sec. Inlet values of kinetic energy and dissipation were varied over a wide range as will be discussed below.

The computational grid was composed of 94 cells in the cross stream direction and 51 in the longitudinal direction. This basic grid was used for most of the study, but was expanded to 94 by 100 for one run to test grid dependency.

EFFECT OF UPSTREAM BOUNDARY CONDITIONS

Initially, a nonunique solution of the steady equations was anticipated as a result of the Coanda effect. To test for the suspected Coanda effect, the central jet was given a positive y component of velocity and a converged solution was obtained. Beginning again from the converged, perturbed solution but with an unperturbed boundary condition, a new solution was calculated. In early runs, a nonunique solution was obtained, but with an unrealistic downstream pressure boundary condition. The length of the calculation domain was so short that a downstream zero pressure boundary condition was physically unrealistic. When the boundary condition was moved farther away from the inlet, the calculated flow appeared to be unique.

Next, a parametric study of changes in upstream boundary conditions on k and ϵ was done. Inlet values for k and ϵ were input according to equations (1) and (2).

$$k_{in} = \text{turb } U_{in}^2 \quad (1)$$

$$\epsilon_{in} = d k_{in}^{3/2} / L \quad (2)$$

In these equations, turb and d were constants, and L is a fixed turbulent length scale. For the k - ϵ model, the effective viscosity is calculated from equation (3).

$$\mu_e = 0.09 \rho k^2 / \epsilon + \mu_1 \quad (3)$$

Here ρ is the fluid density, and μ_1 is the fluid laminar (molecular) viscosity. From the above three equations, if the incoming kinetic energy of turbulence is increased, the incoming viscosity increases as $k^{1/2}$. The effective viscosity affects diffusion of mean energy of the flow. If μ_e increases, one would expect that the diffusion would increase. Increased diffusion means that recirculation zones should decrease. In spite of these expectations, the contrary result was obtained. As the

incoming kinetic energy was increased, the extents of the four recirculation zones increased. This is obviously a computational effect because physically a reduction in the size of the recirculation zones is expected.

The effect described above was eliminated by fixing the incoming value of ϵ at a constant value as the incoming kinetic energy was varied. In this case the correct variation of recirculation length with input kinetic energy was obtained over a fairly broad range of values. Even here some care was necessary.

To illustrate, a class of problems were run in which $turb$ was varied from 0.001 to 0.1. ϵ_{in} was fixed at $191,000 \text{ m}^2/\text{sec}^3$. This value of ϵ_{in} is consistent with high values of incoming kinetic energy. As $turb$ was decreased from 0.1 to 0.01, all four recirculation zones increased in length as expected. A typical set of streamlines for $turb$ in this range is shown in Figure 4.

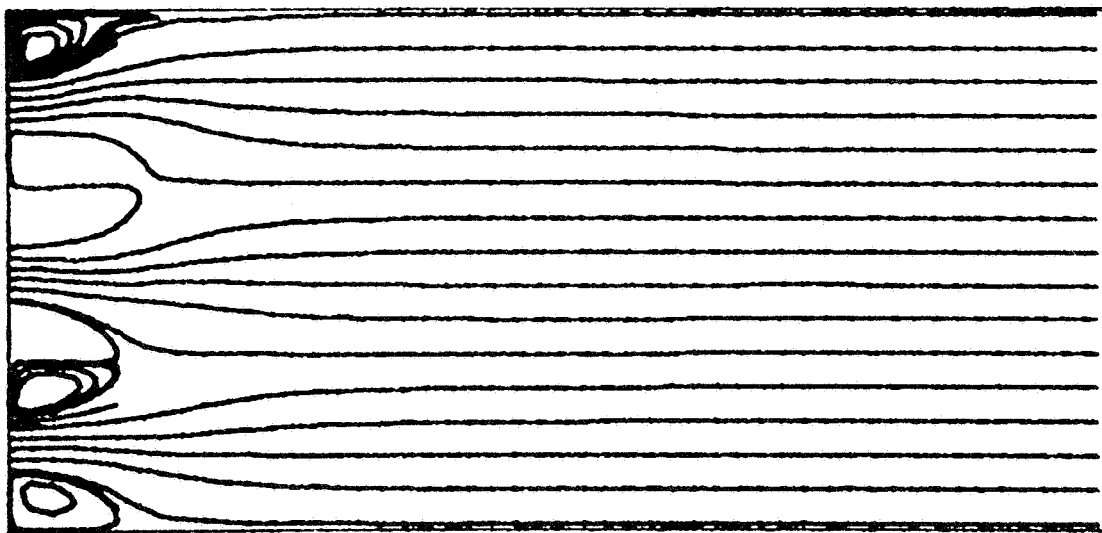


Figure 4. Preburner flow for $turb = 0.01$.

As $turb$ was made smaller than 0.01, an unusual effect was observed. Before, all four recirculation zones (1 to 4 counting from the baffle) remained approximately the same length and increased with decreasing $turb$. When $turb$ was set below 0.01, the result depicted in Figure 5 was obtained. Recirculation zones 1 and 3 were shortened while 2 and 4 remained long. The result was both dramatic and abrupt. Figure 6 depicts the change in recirculation zone length with $turb$. All four curves have similar variation for $0.01 \leq turb \leq 0.1$. For $turb < 0.01$, the curves for zones 2 and 4 reached a maximum limit while the curves for zones 1 and 3 experienced a discontinuous decrease.

This effect was quite stable. An iteration begun with a converged solution for $turb = 0.009$, but with $turb = 0.01$ for the new run, ends up with a solution consistent with $turb = 0.01$. The reverse was also true. As desired, the final solution is sensitive to the boundary conditions but not to the initial guess.

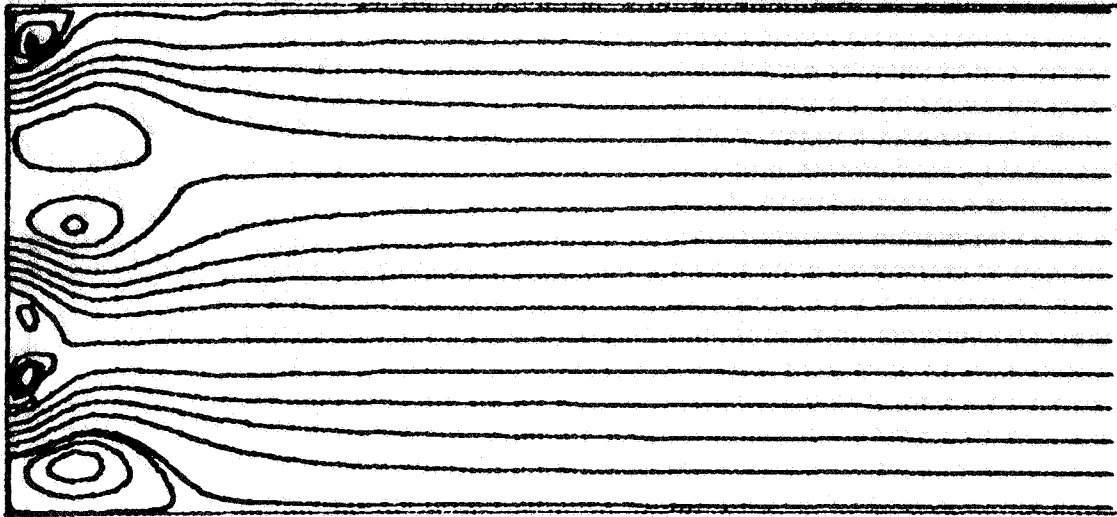


Figure 5. Preburner flow for $turb = 0.001$.

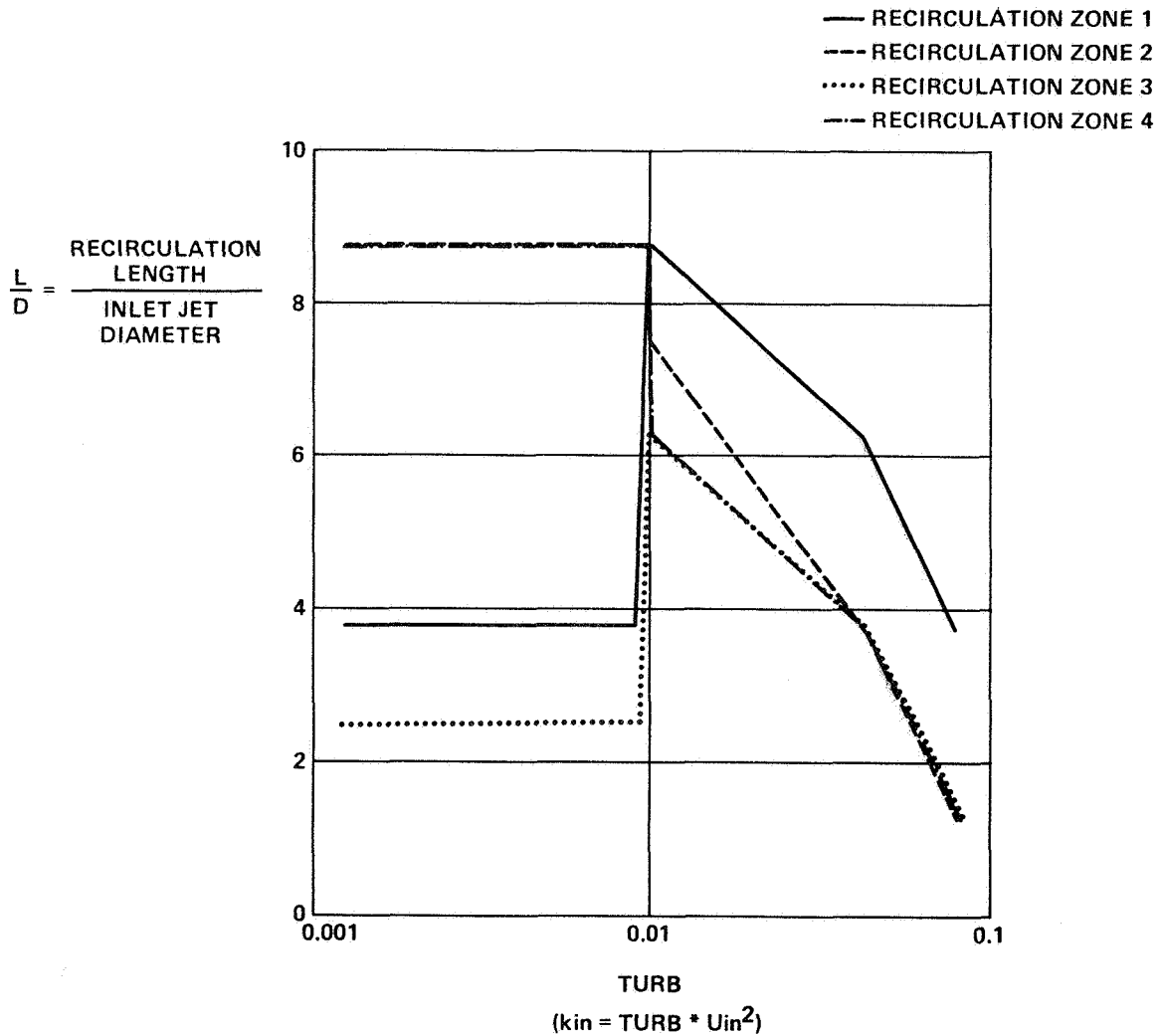


Figure 6. Recirculation zone length as a function of the upstream boundary condition on turbulent kinetic energy.

If the value of ϵ_{in} was decreased to a value consistent with $turb = 0.01$, the discontinuous behavior was no longer observed. The next step in this study is to vary this value of ϵ_{in} over a range and see where the discontinuity begins.

MESH DEPENDENCY

The flow calculations presented above were done with a 94 by 51 mesh. To determine the amount of grid dependency, a mesh 94 by 100 was used. $Turb$ was set at 0.009, and a nonuniform pattern of recirculation zones was observed as before but with one difference. Whereas before the recirculation zones were in the pattern of long-short-long-short, for the refined mesh the pattern was short-long-short-long! Obviously, no claim for grid independence can be made at the present time. Future plans call for finer mesh solutions.

SUMMARY

A two-dimensional model "preburner" was investigated in an attempt to simulate conditions which result in preburner wear in the Space Shuttle Main Engine. For physically realistic conditions, no multiple steady-flow solutions were observed. Wall attachment was observed in every instance. While significant, drawing conclusions about the real preburner based on these results should be done carefully since not all aspects of the flow were included in the simulation, e.g., the coaxial nature of the jets.

A range of phenomena were observed which as yet are poorly understood. The discontinuity and nonuniformity of the recirculation zone lengths is the prime example. If the effect is a physical rather than a numerical phenomenon, then it would have a significant effect on the performance of the preburner. At present no conclusion can be drawn as to whether or not it is a real physical effect.

REFERENCES

1. Patankar, S. V. and Spalding, D. B.: A Calculation Procedure for Heat, Mass, and Momentum Transfer in Three-Dimensional Parabolic Flows. *Int. J. Heat Mass Transfer*, Vol. 15, p. 1787.
2. Launder, B. E. and Spalding, D. B.: The Numerical Computation of Turbulent Flows. *Comp. Meth. in Appl. Mech. Eng.*, Vol. 3, 1974, p. 269.

APPROVAL

A COMPUTATIONAL STUDY OF MULTIPLE JET AND
WALL INTERACTION

By Warren Campbell

The information in this report has been reviewed for technical content. Review of any information concerning Department of Defense or nuclear energy activities or programs has been made by the MSFC Security Classification Officer. This report, in its entirety, has been determined to be unclassified.



G. F. McDONOUGH
Director, Systems Dynamics Laboratory

